PHYSICAL REVIEW B VOLUME 17, NUMBER 5 1 MARCH 1978

Thermoelectric power of nearly magnetic actinide systems*

J. R. Iglesias-Sicardi,† R. Jullien, ‡ and B. Coqblin
Laboratoire de Physique des Solides,§ Université Paris-Sud, Centre d'Orsay 91405 Orsay (France).
(Received 28 December 1976)

The thermoelectric power is computed within the spin-fluctuation theory, with including both the umklapp processes and the possibility of a distorted Fermi surface which are found to be important. The electrical and thermal resistivities are also computed and the effect of umklapp processes is much less important there than in the case of the thermopower. An application of the model to the thermopowers of Pd, Pt, Np, Pu, and UAl_2 is finally presented.

I. INTRODUCTION

It is now well established that the spin-fluctuation theory can account for many properties of neptunium and plutonium metals or of nearly magnetic actinide compounds such as UAl_2, USn_3, $NpRh_3$, $PuRh_2$, and $PuAl_2$.[1] In the spin-fluctuation model used for actinide systems, the conduction electrons of a broad-band are scattered by the spin fluctuations formed by the interacting electrons of a very narrow i band (for example, the f band of an actinide metal) and the temperature dependence of the Stoner susceptibility of the i band is explicitly taken into account because of its relatively small Fermi energy.[2] The electrical resistivity[2] and the thermal conductivity[3] have been previously computed within this model. The electron-paramagnon electrical resistivity starts as T^2 at low temperatures and saturates at high temperatures; the resistivity may go through a maximum or not at intermediate temperatures, which can well account for the resistivity of plutonium or neptunium metals and of some U and Pu compounds. Similarly, the electron-paramagnon thermal resistivity, after the low-temperature-enhanced linear T behavior, goes through a maximum around the spin-fluctuation temperature and then decreases as $1/T$ at higher temperatures. A rough agreement with the experimental thermal conductivity of plutonium[4] has been obtained, but a more quantitative fit is difficult to perform since the spin-fluctuation and the phonon contributions are typically of the same order of magnitude in the case of plutonium.

The third transport property which can be computed within the spin-fluctuation model is the thermoelectric power. The Seebeck coefficients of thorium,[5] uranium,[5] neptunium,[5] plutonium,[6] and UAl_2,[7] have been experimentally determined: the Seebeck coefficients of thorium and uranium are rather small and lying between -5 and $+5\mu V/K$, while the values of neptunium, plutonium, and UAl_2 are much larger, as shown in Fig. 7. The fact that the thermopowers of Np, Pu, and UAl_2 are much larger than those of Th and U is clearly the signature of the presence of spin fluctuations, exactly as in the case of the electrical and thermal resistivities. Similarly, as shown in Fig. 6, the thermopower of exchange-enhanced transition metals, i.e., Pd and Pt, are negative and have a large absolute value at high temperatures. Concerning the thermal dependence, the thermopowers of Pu and UAl_2 are negative at very low temperatures become then positive and saturate at high temperatures.

The thermopower is computed here within the same spin-fluctuation model, but, if we anticipate the results, we can say that the thermopower is always negative and almost linear in temperature within the previously developed model, which takes into account only normal processes. On the other hand, it is well known that the umklapp processes play a very important role in the thermopower due to phonons, in contrast to the case of the electrical and thermal resistivities.

So, the purpose of the present paper is to compute the transport properties within the same spin-fluctuation model involving two parabolic bands, but with now including the umklapp processes and a possible distortion of the Fermi surface with respect to the case of a sphere. Thus, we will firstly derive the thermoelectric power where large effects due to the umklapp processes are expected and then we will compute the relatively weaker effect of umklapp processes on the electrical and thermal resistivities.

II. SPIN-FLUCTUATION MODEL FOR UMKLAPP PROCESSES

A. General points of the model

Before discussing the particularities introduced by the consideration of the umklapp processes in the scattering of an electron by a paramagnon, let us recall the main assumptions and notations of the model.[2]

We use the classical paramagnon model[8]: The con-

duction electrons (labeled by the index c) of a broad-band are scattered by large spin fluctuations formed by the strongly interacting electrons (labeled by the index i) of another very narrow band. The Fermi temperature T_{F_c} of the conduction band is assumed to be much larger than all the usual temperatures, but the Fermi temperature T_{F_i} of the interacting i band can be within the usual temperature range.

The c and i bands are assumed to be parabolic and we will use the following notations: ν is the number of atoms per unit volume, while $k_{F_\alpha}=(3\pi^2 n_\alpha)^{1/3}$, $N_\alpha(\epsilon_{F_\alpha})=m_\alpha^* k_{F_\alpha}/\pi^2\nu$, m_α^* and n_α (with α equal to c or i) are, respectively, the Fermi momentum at $T=0$, the density of states per atom at the Fermi level, the effective mass, and the number of α electrons per unit volume. J is the coupling constant between electrons of the two bands. Finally, we make $\hbar=k_B=1$ in the calculations.

The spin-fluctuation spectrum $\mathrm{Im}\chi(q,\omega,T)$ is the imaginary part of the dynamical paramagnetic susceptibility of the interacting i electrons given by the random-phase approximation (RPA):

$$\chi(\vec{q},\omega,T)=\chi^0(\vec{q},\omega,T)/[1-I\chi^0(\vec{q},\omega,T)] \quad . \tag{1}$$

$\chi^0(\vec{q},\omega,T)$ is the i susceptibility without the interaction I:

$$\chi^0(\vec{q},\omega,T)=\sum_{\vec{k}}\frac{f(\epsilon_{\vec{k}},T)-f(\epsilon_{\vec{k}+\vec{q}},T)}{\epsilon_{\vec{k}+\vec{q}}-\epsilon_{\vec{k}}-\omega} \quad . \tag{2}$$

The approach to magnetism is quantitatively described by the Stoner enhancement factor:

$$S=1/[1-I\chi^0(0,0,0)]=1/(1-\bar{I}) , \tag{3}$$

which diverges at the ferromagnetic instability

$$I\chi^0(0,0,0)=\tfrac{1}{2}IN_i(\epsilon_{F_i})=\bar{I}=1 \quad .$$

In the spin-fluctuation model, we have taken into account the full T dependence of the Fermi distribution $f(\epsilon_{\vec{k}},T)$, by keeping constant the total number of i electrons:

$$\sum_{\vec{k}} f(\epsilon_{\vec{k}},T)=n_i/2\nu \quad . \tag{4}$$

So, for a given i band, the shift of the Fermi level may be computed implicitly and, assuming I to be constant, the thermal variation of the spin-fluctuation spectrum is deduced and then the electrical[2] and thermal[3] resistivity curves are derived in the case of normal processes.

B. Approximations used for the treatment of the umklapp processes

The preceding calculations of the electrical[2] and thermal[3] resistivities are valid only if the radius k_{F_c} of the conduction-electron Fermi sphere is much smaller than the dimension of the Brillouin zone. But, in the scattering process of the electrons by paramagnons, we have in general the relation

$$\vec{K}=\vec{k}'-\vec{k}=\vec{q}+\vec{G} \tag{5}$$

connecting the incoming and outcoming electron wave vectors $\vec{k}$ and $\vec{k}'$ to the paramagnon wave vector $\vec{q}$ and to the reciprocal-lattice vector $\vec{G}$. If $\vec{K}$ lies inside the first Brillouin zone, the scattering process is "normal," which corresponds to $\vec{G}=0$ in the relation (5). On the contrary, if $\vec{K}$ lies outside the first Brillouin zone, we need a nonzero $\vec{G}$ value in order to check the relation (5) and the process is called an "umklapp" one (U process). The geometry of an umklapp process is given in Fig. 1 for a simple-cubic case.

There is presently no calculation including the umklapp processes in the electron-paramagnon scattering, except a very brief attempt by Kaiser[9] to describe the thermopower of nearly magnetic alloys. However, there are similar calculations for the thermoelectric power due to phonons by Ziman[10] and Rösler,[11] and we will use here some of their approximations. Ziman[10] has used the rough approximation of changing the discrete summation over $\vec{G}$ into an angular integration which gives then an integration over $\vec{q}$ and he has taken the maximum q value $q_{\max}$ equal to the radius of the Debye sphere in the Debye model; the approach of Ziman is reasonable in the case of phonons because the Debye radius is in fact a natural cutoff. On the other hand, Rösler[11] has restricted the $\vec{K}$ integration for an umklapp process to values outside the first Brillouin zone and inside the sphere of radius $2k_{F_c}$, but he has taken the pseudopotential form factor of phonons constant and equal to its value at $2k_{F_c}$.

So, for the scattering by paramagnons, we will use the following approximations:

(i) We retain only the normal processes ($\vec{G}=0$) and the umklapp processes corresponding to the smallest nonzero G value; there are consequently Z-equivalent reciprocal-lattice vectors, where Z is the coordination

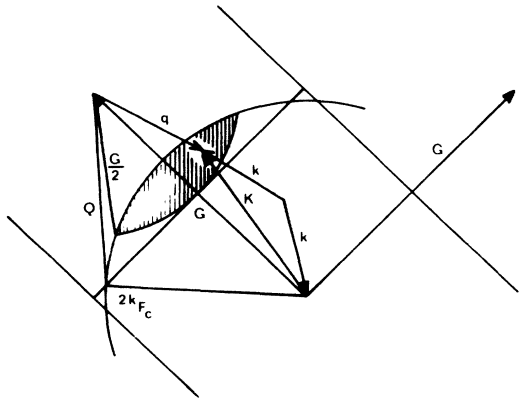

FIG. 1. Geometry of an umklapp process for a simple cubic lattice.

number. However, in the case of small $G/2k_{F_c}$ values, the sphere of radius $2k_{F_c}$ cuts the third Brillouin-zone boundaries and, in principle, we would be obliged to deal with the two different smallest G values; so this effect is neglected here, but it certainly does not modify deeply the physical results.

(ii) In the case of an U process, we will use the Ziman approximation of changing the discrete summation over $\vec{G}$ into an angular integration which gives then an integration over $\vec{q}$. This approximation will be explained in detail in Sec. III.

(iii) To compute the transport properties, we need to integrate over both $\vec{K}$ and $\vec{q}$. For a normal process, we integrate over $\vec{K}=\vec{q}$ from 0 to the maximum q value $q_{\max}$. For an U process, we simplify the calculations by making a spherical integration over both $\vec{q}$ and $\vec{K}$. We firstly integrate over $\vec{K}$ and for a given $|\vec{q}|$ value, the possible $|\vec{K}|$ values lie between $G-q$ and $2k_{F_c}$. Then, the integration over $\vec{q}$ is performed from $q_{\min}$ to $q_{\max}$ and the minimum $q_{\min}$ value of q is obtained for $K=2k_{F_c}$ and $\vec{q}$ parallel to $\vec{G}$, so that we have $q_{\min}=G-2k_{F_c}$.

(iv) The determination of the maximum q value $q_{\max}$ is more delicate and depends on the approximations of the model. There is no natural value for $q_{\max}$ as in the Debye model for phonons. So, we will approximate the first Brillouin zone by a sphere of radius $q_{\max}=\frac{1}{2}G$, so that the domain for the K integration, which corresponds to the shaded area of Fig. 1, lies inside both the sphere of radius $2k_{F_c}$ and the sphere translated by $\vec{G}$ and of radius $\frac{1}{2}G$. This approximation depends obviously on the crystallographic structure and it is in fact a better approximation for a larger coordination number Z of the reciprocal lattice. This approximation gives probably an underestimation of the electrical and thermal resistivities as will be discussed in Sec. IV, but we have checked in this paper that increasing slightly $q_{\max}$ does not modify really the thermal dependence of the transport properties. So, since the crystallographic structure is generally complex in actinide metals and compounds, as, for example, the monoclinic structure of α-Pu and since the band structure is also complicated, the purpose of the present paper is to take a simplified model in order to make possible the study of the umklapp processes in the electron-paramagnon scattering. Thus, in the following, we will perform the calculations for a simple-cubic case ($Z=6$) with $q_{\max}=\frac{1}{2}G$ and for two parabolic c and i bands.

(v) Finally, the proposed limits on $\vec{q}$ only refer to one of the reciprocal-lattice points and for $\vec{q}$ to lie in a sphere surrounding it. Indeed, we must multiply by the coordination number Z to obtain the full average over all orientations of $\vec{k}$ and $\vec{k}'$ in the calculations of the transport properties.

Finally, we do not make any approximation on the spin-fluctuation spectrum and we keep the full q, ω, and T dependence of $\mathrm{Im}\chi(\vec{q},\omega,T)$, which is a very important point for paramagnons and which is obviously better than the constant value of the form factor used for phonons by Rösler.[11]

In Sec. III, we will compute the spin-fluctuation contribution to the thermopower and we will neglect both the phonon contribution and the effects of phonon or "paramagnon drag." It is certainly justified to neglect the phonon contribution, since in the case of the thermopower we add the quantities ρQ, and both the resistivity ρ and the thermopower Q are much smaller for phonons than for paramagnons, as shown by the rapid increase of ρ and Q from Th and U to Np, U, and UAl_2. On the other hand, the effect of "paramagnon-drag" has not really been computed and has been discussed only qualitatively by Kaiser.[9] The effects of phonon and paramagnon drag will be mentioned in Sec. V when comparing the theoretical results to experiments.

III. THERMOELECTRIC POWER

A. Theoretical calculation

According to Ziman,[11] the spin-fluctuation contribution to the thermoelectric power can be written

$$Q=\tfrac{1}{3}\pi^2(k_B/e)(T/T_{F_c})x \quad , \tag{6}$$

where k_B and e are, respectively, the Boltzmann constant and the negative electron charge; x is given by

$$x=x_0\left(1+\frac{\pi^2T^2}{3}\frac{P_{11}}{P_{22}}\right)-T_{F_c}\frac{P_{21}}{P_{22}} \quad . \tag{7}$$

The quantity x_0 depends on the shape of the conduction-electron Fermi surface and is defined for paramagnons as for phonons.[10] The present calculation of the thermoelectric power is performed for a spherical Fermi surface of conduction electrons, so that x_0 is equal to $\frac{3}{2}$. Indeed, the conduction-electron Fermi surface of nearly magnetic actinide systems is different from a sphere and consequently x_0 must be smaller than $\frac{3}{2}$ because x_0, which is equal to $\frac{3}{2}$ for a spherical Fermi surface of electrons, has a smaller value for a distorted Fermi surface, becomes negative if the holes are the most numerous carriers, and reaches finally the value $-\frac{3}{2}$ if the Fermi surface is only a sphere of holes inside the first Brillouin zone. In fact, x_0 can be in principle computed as a function of the ratio $G/2k_{F_c}$ and the relation between x_0 and $G/2k_{F_c}$ depends on both the geometry of the Brillouin zone and the band structure of conduction electrons, but this calculation yields really inextricate calculations and does not seem necessary here since we have not used realistic crystallographic and band structures for actinide systems. So, we will perform the calculation

of the thermopower by assuming a spherical Fermi surface and consequently $x_0=\frac{3}{2}$ and, only at the end of the calculation, we will consider x_0 and $G/2k_{F_c}$ as independent parameters and present some results for different x_0 values, in order to describe tentatively an effect due to a distortion of the conduction-electron Fermi surface.

The method used by Ziman to derive the expression (7) is a variational one and the P_{ij} functions are then given by

$$P_{ij}=\frac{1}{T}\sum_{\vec{G}}\sum_{\vec{k}}\sum_{\vec{k}'}\sum_{\vec{q}} f(\epsilon_{\vec{k}})[1-f(\epsilon_{\vec{k}'})]\int\frac{\mathrm{Im}\chi(\vec{k}'-\vec{k},\omega,T)}{(e^{\omega/T}-1)(1-e^{-\omega/T})}\delta_{\vec{k}-\vec{k}'+\vec{q}+\vec{G}}\delta(\epsilon_{\vec{k}'}-\epsilon_{\vec{k}}-\omega)A_{ij}\,d\omega \quad , \tag{8}$$

where the sum over $\vec{G}$ includes both $G=0$ (N processes) and the smallest nonzero $\vec{G}$ values (U processes). As usual, T and ω stand, respectively, for k_BT and $\hbar\omega$ and the A_{ij} coefficients are given by

$$A_{11}=(\vec{k}'\cdot\vec{u}-\vec{k}\cdot\vec{u})\,(\vec{k}'\cdot\vec{u}-\vec{k}\cdot\vec{u}) \quad , \tag{9a}$$

$$A_{22}=[(\epsilon_{\vec{k}'}-\epsilon_{F_c})\vec{k}\cdot\vec{u}-(\epsilon_{\vec{k}}-\epsilon_{F_c})\vec{k}\cdot\vec{u}]\times[(\epsilon_{\vec{k}'}-\epsilon_{F_c})\vec{k}'\cdot\vec{u}-(\epsilon_{\vec{k}}-\epsilon_{F_c})\vec{k}\cdot\vec{u}] \quad , \tag{9b}$$

$$A_{12}=(\vec{k}'\cdot\vec{u}-\vec{k}\cdot\vec{u})[(\epsilon_{\vec{k}'}-\epsilon_{F_c})\vec{k}'\cdot\vec{u}-(\epsilon_{\vec{k}}-\epsilon_{F_c})\vec{k}\cdot\vec{u}] \quad , \tag{9c}$$

where $\vec{u}$ is an unit vector in the direction of the electric field.

The electrical and thermal resistivities are proportional to, respectively, P_{11} and P_{22} as will be explained in Sec. IV, while the thermopower involves a new function P_{21}. If we call ϵ the energy $\epsilon_{\vec{k}}=k^2/2m_c^*$ and if we introduce the vector $\vec{K}$ given by (5), we obtain immediately

$$A_{11}=\tfrac{1}{3}K^2 \quad , \tag{10a}$$

$$A_{22}=\tfrac{1}{3}[\omega^2k^2+(\epsilon-\epsilon_{F_c})(\epsilon+\omega-\epsilon_{F_c})K^2+2m_c^*\omega^2(\epsilon+\omega-\epsilon_{F_c})] \quad , \tag{10b}$$

$$A_{12}=\tfrac{1}{3}\{\tfrac{1}{2}K^2[2(\epsilon-\epsilon_{F_c})+\omega]+m_c^*\omega^2\} \quad . \tag{10c}$$

Performing the integration over $\vec{k}'$ by use of the Kronecker symbol of (8) and changing the variable $\vec{q}$ to $\vec{K}=\vec{q}+\vec{G}$, give

$$P_{ij}=\frac{1}{T}\sum_{\vec{G}}\sum_{\vec{k}}\sum_{\vec{K}} f(\epsilon_{\vec{k}})[1-f(\epsilon_{\vec{k}+\vec{K}})]\int\frac{\mathrm{Im}\chi(\vec{K},\omega,T)}{(e^{\omega/T}-1)(1-e^{-\omega/T})}\delta(\epsilon_{\vec{k}+\vec{K}}-\epsilon_{\vec{k}}-\omega)A_{ij}\,d\omega \quad . \tag{11}$$

Eliminating the δ function and transforming the summations over $\vec{k}$ and $\vec{K}$ into integrals give then

$$P_{ij}=\frac{1}{T}\sum_{\vec{G}} d\omega\int k\,dk\int K\,dK\,\Theta\left(2k-K+\frac{2m_c^*\omega}{K}\right)\frac{f(\epsilon)[1-f(\epsilon+\omega)]}{(e^{\omega/T}-1)(1-e^{-\omega/T})}\mathrm{Im}\chi(\vec{K},\omega,T)A_{ij} \quad , \tag{12}$$

where $\Theta(k)$ is the Heaviside function.

Making the transformation,

$$\epsilon=\epsilon_{F_c}+Tx \quad , \tag{13}$$

$$\omega=Ty \quad , \tag{14}$$

leaves A_{11} given by (10a) unchanged and transforms A_{22} and A_{12} into

$$A_{22}=\tfrac{1}{3}T^2[y^2k^2+x(x+y)K^2+2m_c^*Ty^2(x+y)] \quad , \tag{15a}$$

$$A_{12}=\tfrac{1}{3}T[\tfrac{1}{2}K^2(2x+y)+m_c^*Ty^2] \quad . \tag{15b}$$

Thus, P_{ij} becomes

$$P_{ij}=m_c^*T\sum_{\vec{G}}\int\frac{dy}{(e^y-1)(1-e^{-y})}\times\int K\,dK\int dx\,\Theta\left(2k-K+\frac{2m_c^*Ty}{K}\right)\times[f(x)-f(x+y)]\mathrm{Im}\chi(\vec{K},Ty,T) \quad . \tag{16}$$

$\Theta(x)$ is the Heaviside function. As usual, we define the integrals

$$I_n(y)=\int x^n[f(x)-f(x+y)]dx \tag{17a}$$

with

$$I_0(y)=y,\quad I_1(y)=-\tfrac{1}{2}y^2,\quad I_2(y)=\tfrac{1}{3}y(y^2+\pi^2) \quad . \tag{17b}$$

Following Rösler,[11] we expand the different functions for a k value near the Fermi value k_{F_c}; in partic-

ular, we can write

$$\Theta\left(2k - K + \frac{2m_c{}^*Ty}{K}\right) \simeq \Theta(2k_{F_c} - K) + 2m_c{}^*T\left(\frac{x}{k_{F_c}} + \frac{y}{K}\right)\delta(2k_{F_c} - K) \quad . \tag{18}$$

Then, we calculate the P_{ll} functions by taking into account the lowest-order term in T in the expression (18) and by changing the summation over the smallest $\vec{G}$ values into an integral. We separate out the sum on $\vec{G}$ into N and U processes; for $G = 0$, the vector $\vec{K}$ is equal to $\vec{q}$ and the expression (16) involves an integral over only y and K. For umklapp processes, the problem is more delicate and, as announced in Sec. II B, we will follow an approximate argument of Ziman[10] to perform the sum on $\vec{G}$ and the integral over K. Ziman considers that it is possible to change the discrete sum on $\vec{G}$ into an integration over the angle made by $\vec{G}$ with a fixed direction, which represents certainly a very rough approximation. If we call ψ the angle between the vectors $\vec{G}$ and $\vec{K}$, we write

$$q^2 = G^2 + K^2 - 2GK\cos\psi \quad , \tag{19}$$

So, using the approximation of Ziman, we change the sum on $\vec{G}$ into an integration on ψ with keeping G and $\vec{K}$ fixed and finally the integration on ψ is changed to an integration on $\vec{q}$, with the element of integration $\sin\psi\, d\psi = q\, dq\, /GK$.

As previously explained in Sec. II B, we use the limits of integration for K and q and we multiply the result by the coordination number Z; so, the expression (16) involves an integral over y, K, and q for U processes.

So, P_{11} and P_{22} become

$$P_{11} = \frac{m_c{}^*T}{3}k_{F_c}^4 \int_0^\infty \frac{y\, dy}{(e^y - 1)(1 - e^{-y})} A_3(yT) \quad , \tag{20}$$

$$P_{22} = \frac{m_c{}^*T^3}{3}k_{F_c}^4 \times \int_0^\infty \frac{y^3A_1(yT) + \frac{1}{3}\pi^2 yA_3(yT) - \frac{1}{6}y^3A_3(yT)}{(e^y - 1)(1 - e^{-y})}\, dy \quad , \tag{21}$$

where the function $A_n(\omega)$ are the sums of a contribution $A_n^N(\omega)$ from normal processes and a contribution $A_n^U(\omega)$ from umklapp processes, i.e.:

$$A_n(\omega) = A_n^N(\omega) + A_n^U(\omega) \quad , \tag{22}$$

where we have for $G = 0$

$$A_n^N(\omega) = \frac{1}{(k_{F_c})^{n+1}} \int_0^{G/2} q^n \mathrm{Im}\chi(\vec{q}, \omega, T)\, dq; \tag{23}$$

and for $G \neq 0$

$$A_n^U(\omega) = \frac{Z}{G(k_{F_c})^{n+1}} \times \int_{G-2k_{F_c}}^{G/2} q\, dq \int_{G-q}^{2k_{F_c}} K^{n-1}\mathrm{Im}\chi(\vec{K}, \omega, T)\, dK \tag{24}$$

If similarly we retain only the lowest-order terms of (18), P_{12} is strictly equal to zero since the integral over q is proportional to $2I_1(y) + yI_0(y)$ which is zero according to (17b). So we need to evaluate P_{12} to an higher-order term in T, i.e., to consider the second term of (18). So, P_{12} can be written

$$P_{12} = \frac{m_c{}^{*2}T^3}{3}\sum_{\vec{G}}\left[\int_0^\infty \frac{y^2I_0(y)\,dy}{(e^y - 1)(1 - e^{-y})}\int K\, dK\, \Theta(2k_{F_c} - K)\,\mathrm{Im}\chi(\vec{K}, Ty, T) + \int_0^\infty \frac{dy}{(e^y - 1)(1 - e^{-y})}\int K^3\, dK\,\mathrm{Im}\chi(\vec{K}, Ty, T)\delta(2k_{F_c} - K) \times \left[\frac{2I_2(y)}{k_{F_c}} + \frac{2yI_1(y)}{K} + \frac{yI_1(y)}{k_{F_c}} + \frac{y^2}{K}\right]\right] \quad . \tag{25}$$

The first term of (25) can be evaluated approximately by the method previously used for computing P_{11} and P_{22}. The second term of (25) can be calculated exactly because of the presence of the δ-function and its value is independent of the nature of the scattering processes, because K can always be equal to $2k_{F_c}$ either by N processes (when the sphere of radius $2k_{F_c}$ is inside the first Brillouin zone) or by U processes (when the sphere of radius $2k_{F_c}$ is outside the first Brillouin zone).

So, finally the expression (25) becomes

$$P_{12}=\tfrac{1}{3}(m_c{}^*k_{F_c}T)^2\left[\int_0^\infty \frac{y^3A_1(yT)\,dy}{(e^y-1)(1-e^{-y})}+\frac{4}{3}\int_0^\infty \frac{y(y^2+4\pi^2)}{(e^y-1)(1-e^{-y})}\,\mathrm{Im}\chi(2k_{F_c},Ty,T)\,dy\right] . \tag{26}$$

So, by use of the expressions (22)–(24), x given by (7) becomes equal to

$$x=x_0+\alpha/\beta , \tag{27}$$

where

$$\alpha=\int_0^\infty \frac{dy}{(e^y-1)(1-e^{-y})}\left[\tfrac{1}{3}\pi^2x_0yA_3(Ty)-\tfrac{1}{2}y^3A_1(Ty)-\tfrac{2}{3}y(y^2+4\pi^2)\mathrm{Im}\chi(2k_{F_c},Ty,T)\right] , \tag{28}$$

$$\beta=\int_0^\infty \frac{dy}{(e^y-1)(1-e^{-y})}\left[y^3A_1(Ty)+\tfrac{1}{3}\pi^2yA_3(Ty)-\tfrac{1}{6}y^3A_3(T)\right] . \tag{29}$$

The thermoelectric power is finally given by (6) using (27)–(29).

B. Theoretical results

The theoretical results for the thermopower Q are presented versus the reduced temperature T/T_{F_i} for several parameters: the exchange-enhancement factor S, $\xi=k_{F_c}/k_{F_i}$, $\lambda=G/2k_{F_c}$, and x_0. Indeed, as previously explained, a variation of x_0 is not consistent with the whole calculation which is performed for a spherical Fermi surface, however it gives certainly a good description of the variation of the thermopower with the distortion of the Fermi surface. We may vary the parameter λ from 1 to 2, because for $\lambda\geq 2$ the sphere of radius $2k_{F_c}$ is inside the first Brillouin zone and for $\lambda\leq 1$ the Fermi surface cannot be really described by a sphere.

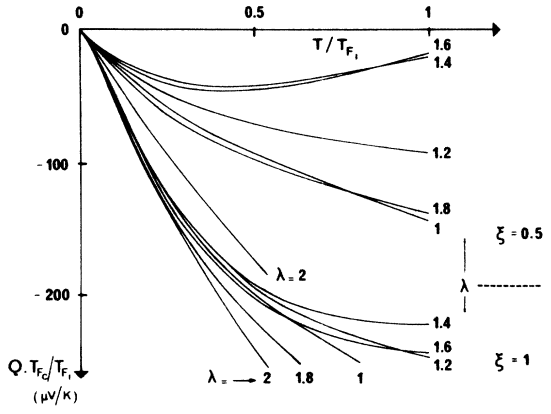

FIG. 2. Theoretical plots of QT_{F_c}/T_{F_i} vs T/T_{F_i}, where Q, T_{F_c}, and T_{F_i} are, respectively, the thermoelectric power, and the c and i Fermi energies. The curves are drawn for several $\xi=k_{F_c}/k_{F_i}$ and $\lambda=G/2k_{F_c}$ values and for $S=10$, $Z=6$, and $x_0=\frac{3}{2}$.

Figures 2 and 3 give the main theoretical results of QT_{F_c}/T_{F_i} vs T/T_{F_i} for $S=10$, $Z=6$ (case of a simple-cubic structure), and several ξ, λ, and x_0 values. Figure 2 gives the results for a spherical Fermi surface ($x_0=\frac{3}{2}$) and Fig. 3 gives the results for several x_0 values in the case $\lambda=1$, for which the Fermi surface is certainly distorted from a sphere.

Let us firstly summarize the results for the case of normal processes only, with a spherical Fermi surface:

(i) The value of x is always positive and does not depend very much on temperature, so that Q is always negative and almost linear with temperature.

(ii) The main effect on the thermopower comes from the crystallographic and band structures through ξ, λ, and x_0, rather than directly from the enchange-enhancement factor S; this effect was already present at a minor degree in the case of the resistivity. In the present case, S appears equally in the numerator α and the denominator β of (27), so that the thermopower is almost completely independent of S. The

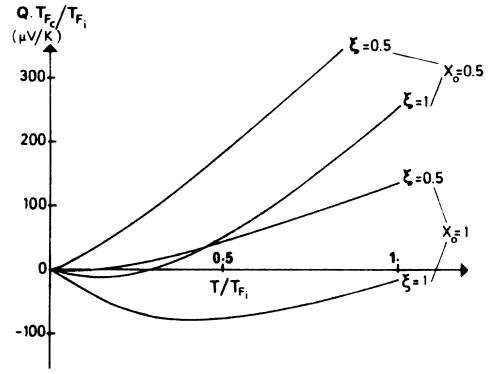

FIG. 3. Theoretical plots of QT_{F_c}/T_{F_i} vs T/T_{F_i}, where Q, T_{F_c}, and T_{F_i} are, respectively, the thermoelectric power, and the c and i Fermi energies. The curves are drawn for several $\xi=k_{F_c}/k_{F_i}$ and x_0 values and for $S=10$, $Z=6$, and $\lambda=1$.

same effect is observed for the Lorenz number[3] where S appears equally in the electrical and thermal resistivities, leading to an almost S-independent Lorenz number. So, in the case of nearly magnetic actinide systems, the spin fluctuations do not contribute really to the thermal dependence of the thermopower, while they are important for the resistivity; however, a large contribution to the thermopower is obtained because T_{F_i} is taken as relatively small as for the electrical and thermal resistivities.

(iii) The thermopower does not vary very much with ξ, as it can be easily seen on Fig. 2 for $\xi=1$ and $\xi=0.5$.

(iv) If we take a ratio T_{F_c}/T_{F_i} of order 20, the absolute value $|Q|$ reaches at $T=T_{F_i}$ a large value of order 20 μV/K.

The introduction of both the umklapp processes and the distortion of the conduction-electron Fermi surface yields important modifications of the thermopower, while, as we will see in Sec. IV, the electrical and thermal resistivities are not really modified by the introduction of U processes.

As previously done for the electrical and thermal resistivities,[2,3] we have computed here the high-temperature expansion of x by use of relations on $\chi(\vec{q},\omega,T)$ and we have shown that x tends at high temperatures to a constant x given by

$$x_\infty = 2x_0 - 2/[\tfrac{1}{16}\lambda^4 + Z(1+\tfrac{1}{80}\lambda^4 - \tfrac{1}{2}\lambda - 2/5\lambda)] \ . \quad (30)$$

So, the asymptotic value x_∞ depends on the crystallographic and band structure by Z, λ, and x_0. For $\lambda=2$ (N processes), x_∞ is equal to $2(x_0-1)$, i.e., 1 for $x_0=\frac{3}{2}$; x_∞ decreases when λ decreases from 2, then goes to a negative minimum value for λ of order 1.5 and increases finally to reach, for $\lambda=1$, a x_∞ value smaller than the x_∞ value obtained for $\lambda=2$.

The main results of the total thermopower due to both N and U processes can be summarized as follows:

(i) First, there is a drastic effect of the U-processes for $x_0=\frac{3}{2}$. We see in Fig. 2 that the thermopower, although remaining always negative, has a clear positive curvature when λ differs from 2 and even goes through a minimum when λ is close to 1.5.

(ii) Second, there is also a drastic effect of a distortion of the conduction-electron Fermi surface. The results are plotted in Fig. 3 for several x_0 values and for $\lambda=1$, because, when λ is close to 1, the Fermi surface is certainly distorted from a sphere. We see in Fig. 3 that, for $x_0=\frac{1}{2}$, we obtain a curve changing sign with temperature or even a curve which is always positive. Moreover, if a negative x_0 value had been chosen, we would have found a very large and positive thermopower. However, the curvature of the different curves is always positive and we cannot obtain at present a positive and saturating thermopower.

(iii) We observe that the thermopower curves for λ different from 2 are closer to the $\lambda=2$ curve at low temperatures than at high temperatures, indicating that the U processes are more efficient at high temperatures, as expected.

(iv) The thermopower is almost completely independent of the exchange-enhancement factor as discussed in the case of N processes only, so that all the curves have been drawn for $S=10$.

(v) The thermopower does not vary very much with ξ, although the variation with ξ is much more important for U processes than for N processes. Moreover, according to (30), the high-temperature slope of the Q vs T curves is independent of ξ, as it can be seen in Fig. 3.

(vi) If we take a ratio T_{F_c}/T_{F_i} of order 20, we obtain values of Q ranging at $T=T_{F_i}$ between -20 to $+20$ μV/K, according to the different parameters of Figs. 2 and 3. Thus the Q values are relatively large at $T=T_{F_i}$ and if we take relatively small T_{F_i} values, as generally done in the case of nearly magnetic actinides,[1,2] we obtain large thermopower values.

IV. ELECTRICAL AND THERMAL RESISTIVITIES

A. Theoretical calculations

We have shown in Sec. III that the umklapp processes play an important role in the thermopower and we will study here their role in the electrical and thermal resistivities.

The electrical and thermal resistivities are, respectively, connected to P_{11} and P_{22} by the following relations:

$$\rho/\rho_0 = (9n_i/2m_c{}^*k_{F_c}^4\,\nu)P_{11} \ , \quad (31)$$

$$\frac{W}{\rho_0/L_0T_{F_i}} = \frac{27n_i}{2\pi^2 m_c{}^*k_{F_c}^4\,\nu T^3}P_{22} \ , \quad (32)$$

where

$$\rho_0 = [\tfrac{1}{4}JN_c(\epsilon_F)]^2\frac{m_c{}^*T_{F_c}}{n_c e^2}\frac{\nu}{n_c} \ , \quad (33a)$$

$$L_0 = \frac{\pi^2 k_B^2}{3e^2} \ , \quad (33b)$$

so that we can write

$$\rho = \frac{\rho_0}{T}\int_0^\infty \frac{\omega A_3(\omega)\,d\omega}{(e^{\omega/T}-1)(1-e^{-\omega/T})} \ , \quad (34)$$

$$W=\frac{\rho_0}{L_0 T^4}\int_0 \frac{\omega T^2 A_3(\omega)+(3/\pi^2)\omega^3 A_1(\omega)-(1/2\pi^2)\omega^3 A_3(\omega)}{(e^{\omega/T}-1)(1-e^{-\omega/T})}\,d\omega\ . \tag{35}$$

B. Theoretical results

Figures 4 and 5 give typical plots of the electrical and thermal resistivities versus T/T_{F_i} for a spherical Fermi surface, $S=10$, $Z=6$ and for several values of $\lambda=G/2k_{F_c}$ and $\xi=k_{F_c}/k_{F_i}$.

The high-temperature behavior of the electrical resistivity ρ has been also determined and is equal to

$$\rho=\rho'_\infty\,[1+\tfrac{2}{3}(\bar{I}-\tfrac{4}{3}\xi^2)\,T_{F_i}/T]\ , \tag{36}$$

where

$$\rho'_\infty=\rho_\infty[\tfrac{1}{16}\lambda^4+Z(1+\tfrac{1}{80}\lambda^4-\tfrac{1}{2}\lambda-2/5\lambda)]\ , \tag{37}$$

$$\rho_\infty=2\pi\rho_0 n_i/\nu\ . \tag{38}$$

The main results of the electrical resistivity calculation can be summarized as follows:

(i) The general form of the electrical resistivity curves is exactly the same here as in the previous calculation which does not consider the U processes,[2] the only difference being the asymptotic value of the resistivity at high temperatures. In particular, there is the same dependence of ρ on the two parameters S and ξ and the conditions for the existence of a maximum are not modified by the introduction of the U processes, as it can be easily seen in formula (36). So, the effect of U processes is not physically important for the resistivity and all the conclusions of the previous paper[2] on the resistivity remain valid.

(ii) The resistivity is smaller for λ different from 2 than for $\lambda=2$. When, for a fixed k_{F_c} value, λ or G decrease, small regions outside the first Brillouin zone, such as the shadded area shown on Fig. 1, are created for the q integration and the resistivity decreases for the two following reasons: first, we change the q integration involving large q values from $\frac{1}{2}G$ to $2k_{F_c}$ to another q integration involving smaller q values from $G-2k_{F_c}$ to $\frac{1}{2}G$; second, we neglect small portions for the q integration, namely, the regions inside the sphere of radius $2k_{F_c}$ and outside the regions equivalent to the shadded area of Fig. 1. So, the effect resulting from the approximation of taking $q_{\max}=\frac{1}{2}G$ is hidden by the first effect and we see here that the choice of $q_{\max}=\frac{1}{2}G$ is not so crucial.

(iii) The contribution of the U processes increases with temperature for a given λ value. In particular, the low-temperature resistivity T^2 law is due practically only to N processes, while the U processes become important at higher temperatures.

Similarly, the high-temperature behavior of the thermal resistivity W has been computed and is given by

$$W=W'_\infty\,T_{F_i}/T\ , \tag{39}$$

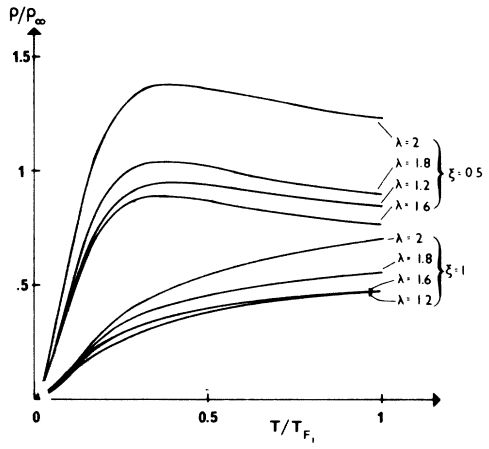

FIG. 4. Theoretical plots of ρ/ρ_∞ vs T/T_{F_i} where ρ, ρ_∞, and T_{F_i} are, respectively, the electrical resistivity, its high-temperature limit, and the i Fermi energy. The curves are drawn for several $\xi=k_{F_c}/k_{F_i}$ and $\lambda=G/2k_{F_c}$ values and for $S=10$, $Z=6$.

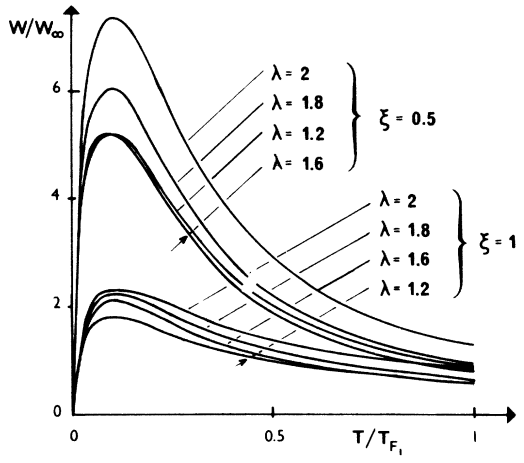

FIG. 5. Theoretical plots of W/W_∞ vs T/T_{F_i}, where W, W_∞, and T_{F_i} are, respectively, the thermal resistivity, the coefficient of its high-temperature T^{-1} law, and the i Fermi energy. The curves are drawn for several $\xi=k_{F_c}/k_{F_i}$ and $\lambda=G/2k_{F_c}$ values and for $S=10$, $Z=6$.

where

$$W'_\infty = \rho'_\infty / L_0 T_{F_i} \ . \tag{40}$$

The main results of the thermal resistivity curves are exactly the same here as in the previous calculation which does not consider the U processes,[3] the only difference being the coefficient W'_∞ of the asymptotic $1/T$ law at high temperatures. The dependence on S and ξ is the same as previously[3] and in particular the temperature of the maximum does not vary with the value of λ. The thermal resistivity is smaller for λ different from 2 than for $\lambda = 2$, for the same reasons as for the electrical resistivity.
The contribution of the U processes increases with temperature, as for the electrical resistivity.

Thus, the conclusions of the previous papers on the electrical[2] and thermal[3] resistivities are not modified by the introduction of the U processes, in contrast to the case of the thermoelectric power.

V. COMPARISON WITH EXPERIMENTS AND CONCLUDING REMARKS

We will compare now the preceding theoretical results to the experimental transport properties of nearly magnetic metals. Since it is difficult to compute the different parameters λ and x_0 for the different nearly magnetic systems, we will present here only a qualitative comparison with experiment in the only case of the thermoelectric power. Concerning the electrical and thermal resistivities, it is clear from Sec. IV that the introduction of the umklapp processes does not modify the main results and all the conclusions of the previous papers[1-3] remain unchanged. In particular, the electrical resistivities of Np and Pu metals or of many uranium and plutonium compounds,[1] as well as the thermal resistivities of Pu[4] or UAl_2[7] can be accounted for by the spin-fluctuation theory and the introduction of the umklapp processes changes only slightly the parameters used for the different fits without modifying really the physical results.

The only available data for the thermoelectric power of nearly magnetic systems concern Pt,[12] Pd,[12] Np,[5] Pu,[6] and UAl_2.[7] The thermoelectric power of platinum and palladium is negative except at low temperatures and reaches values of order -30 or -40 μV/K at very high temperatures, as shown on Fig. 6. In the case of nearly magnetic transition metals, the broad-band c is the s band and the narrow band i is the d band. Thus, the experimental curves of Fig. 6 could be accounted for by the curves of Fig. 2 obtained for $x_0 = \frac{3}{2}$, $S = 10$, λ close to 1 or 2, $\xi = 1$, T_{F_i} of order 1500–2000 K and T_{F_c}/T_{F_i} of order 10, i.e., T_{F_i} and T_{F_c} of order, respectively, 0.15–0.2 and 1.5–2 eV. Let us remark that the values of S, ξ, and T_{F_i} are the same as those used previously to fit the resistivity of palladium.[2] Moreover, the value of T_{F_i}, which is much larger for palladium than for actinide systems, is certainly reasonable here, since the distance between the Fermi energy and the top of the d band is small because there is only 0.5 hole in the d band of Pd; however, the d band of Pd is certainly far from a parabolic band. We can also remark that $|Q|$ is large at high temperatures, which agrees with the large theoretical values that we can obtain in the spin-fluctuation model. Finally, the positive peaks observed at low temperatures could be attributed to an effect either of "paramagnon-drag"[9] or of "phonon-drag".[12]

Figure 7 shows the experimental curves for the thermoelectric power of neptunium,[5] plutonium,[6] and UAl_2.[7] The thermopower of Pu and UAl_2 is negative at low temperatures, changes sign at roughly 30–40 K and shows a clear tendency to saturation at high temperatures. To compare these results to theory, we consider that the i band of these nearly magnetic actinide systems is the very narrow $5f$ band, that the c band is formed by the $7s$ and $6d$ bands and that the d-f hybridization is neglected here. The experimental thermopower of Pu and UAl_2 cannot be fitted by the curves of Figs. 2 and 3, since we have never found a positive thermopower saturating at high temperatures. However, we can qualitatively account for the curves of Fig. 7 by the theoretical curves of Fig. 3 with x_0 smaller than $\frac{3}{2}$, indicating, as expected, that the conduction-electron Fermi surface of Pu and UAl_2 is certainly different from a sphere. The thermoelectric power of plutonium can be reasonably compared to the curve $x_0 = 0.5$, $\xi = 1$, and $S = 10$ of Fig. 3 with T_{F_i}

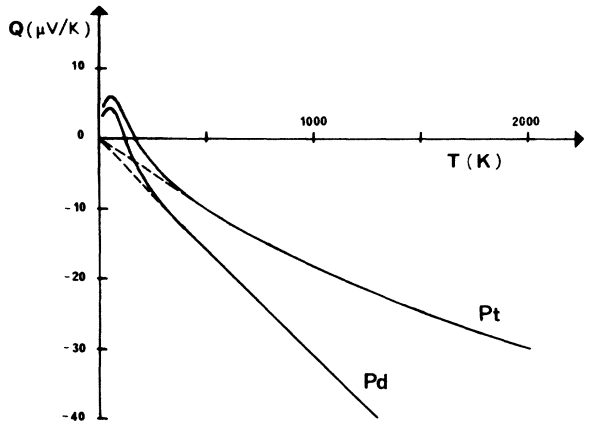

FIG. 6. Experimental plots of the thermoelectric powers of Pt and Pd vs temperature.

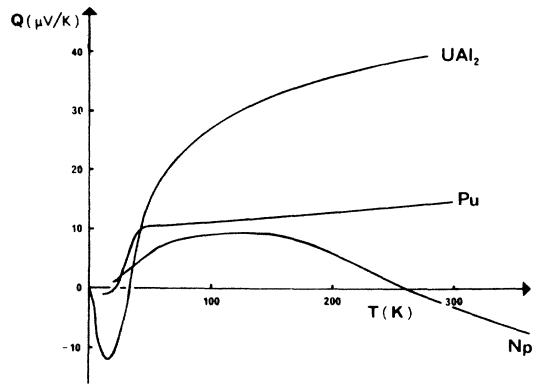

FIG. 7. Experimental plots of the thermoelectric powers of Np, Pu, and UAl_2 vs temperature.

of order 300 K and T_{F_c}/T_{F_i} of order 20, but the theoretical curve is linear instead of presenting a saturation at high temperatures. A similar comparison can be done for UAl_2. However, the negative values of the thermopower observed at low temperatures, in particular the negative peak of UAl_2, are perhaps due to another phenomenon such as the phonon or the paramagnon drag. The thermopower of neptunium is more difficult to be accounted for by the theoretical Figs. 2 and 3. A value for T_{F_i} of 750 K had been previously used to fit the resistivity of neptunium[2] and we need to know the thermopower of Np above 300 K before comparing reasonably the data to theory. However, a possible explanation could be that the negative value of Q above 250 K would correspond to a curve of Fig. 2 and that the positive broad maximum below 250 K would be due to another phenomenon such as the paramagnon drag. So, we have much less succeeded in fitting the thermopowers of nearly magnetic metals than previously their electrical resistivities; however, the general shape and the order of magnitude seem to indicate that the thermopowers of Pd, Pt, Np, Pu, and UAl_2 are essentially due to spin fluctuations.

But it is clear that the present calculation, which is at our knowledge the first detailed one of the spin-fluctuation contribution to the thermopower, must be considered as a first calculation which must be improved, because this approach considers two parabolic c and i bands, treats approximately the umklapp processes and neglects both the phonon contribution and the phonon- or paramagnon-drag effects. However, this calculation is theoretically better than previous calculations on the phonon thermopower[11] since we take into account here the full q, ω, and T dependence of $\chi(q, \omega, T)$.

The preceding calculation must be improved, in particular to obtain a x value passing through a negative minimum and increasing then rapidly with temperature, in order to account for the tendency to saturation observed in Pu and UAl_2 at high temperatures. We can propose at least three possible improvements: first, it would be necessary to have a better description of the umklapp processes and in particular to not use the Ziman approximation; an exact numerical calculation although very long and tedious, is in principle possible to describe correctly the geometry of Fig. 1. The second possible improvement would be to have a better description of the c- and i-band structure; the first step would be to compute x_0 as a function of λ for a given geometry of the Brillouin zone and for a given model for the conduction electrons and then the next step would use more realistic band calculations. The third improvement would be to compute the paramagnon-drag effects which are certainly important at low temperatures.[9] All these improvements would probably yield a positive thermopower saturating at high temperatures as in Pu and UAl_2. The second improvement of considering more realistic band structures is very important and in fact more important here than in the previous calculations of the electrical and thermal resistivities, because the thermopower is very sensitive on the details of the Fermi surface and less dependent on the exchange enhancement factor of the magnetic susceptibility.

At last, in spite of the approximations of the model, both the general form and the order of magnitude of the thermopowers of nearly magnetic metals can be described by the spin-fluctuation model with including the umklapp processes and a distortion of the conduction-electron Fermi surface.

ACKNOWLEDGMENTS

We would like to thank Dr. F. Steglich for giving us his data prior to publication and for very fruitful discussions. One of us (J.R.I.S.) would like to acknowledge Professor J. Friedel and the Laboratoire de Physique des Solides at Orsay for their hospitality during this work.

---

*Part of a Doctorat d'Etat Thesis, submitted on January 10, 1977 by J. R. Iglesias-Sicardi at the Université Paris-Sud, Centre d'Orsay.

†Present address: Instituto de Fisica, U.F.R.G.S., Porto Alegre, Brasil.

‡Present address: Hansen Lab. Department of Applied Physics, Stanford University, Stanford, California 94305.

§Laboratoire associe' au CNRS.

[1]See, for example, R. Jullien and B. Coqblin, in *Plutonium and other Actinides,* edited by H. Blank and R. Lindner, (North-Holland, Amsterdam, 1976), and references therein.

[2]R. Jullien, M. T. Béal-Monod, and B. Coqblin, Phys. Rev. Lett., 30, 1057 (1973); and Phys. Rev. B 9, 1441 (1974).

[3]R. Jullien and B. Coqblin, J. Low Temp. Phys. 19, 59 (1975).

[4]J. F. Andrew, J. Phys. Chem. Solids 28, 577 (1967); R. O. A. Hall and J. A. Lee, Plutonium 1970, edited by W. N Miner (unpublished), p. 35.

[5]G. T. Meaden, Proc. R. Soc. A 276, 553 (1963).

[6]R. Lallement, J. Phys. Chem. Solids 24, 1617 (1963).

[7]F. Steglich (private communication).

[8]A. B. Kaiser and S. Doniach, Int. J. Magn. 1, 11 (1970).

[9]A. B. Kaiser, AIP Conf. Proc. 29, 364 (1976).

[10]J. M. Ziman, in *Electrons and Phonons* (Oxford U.P., New York, 1960).

[11]M.Rösler, Phys. Status Solidi 37, 391 (1970).

[12]R. P. Huebener, in *Solid State Physics,* edited by F. Seitz and D. Turnbull (Academic, New York, 1972), Vol. 27, p. 63.